

# An *in Vitro* Application of Diode Laser-Ozone Based Photodynamic Therapy for Microbial Inactivation

Deny Arifianto<sup>1,2</sup>, Suryani Dyah Astuti<sup>1\*</sup>, Riries Rulaningtyas<sup>1</sup>, Aulia Haidar Rahman Nugraha<sup>1</sup>, Ahmad Khalil Yaqubi<sup>3</sup>, and Ardiansyah Syahrom<sup>4</sup>

<sup>1</sup> Department of Physics, Faculty of Science and Technology, Airlangga University, Surabaya 60115, Indonesia

<sup>2</sup> Department of Engineering, Faculty of Vocational, Airlangga University, Surabaya 60286, Indonesia

<sup>3</sup> Center for Biomedical Research, National Research and Innovation Agency (BRIN), Cibinong, Jawa Barat 16912, Indonesia

<sup>4</sup> Medical Devices and Technology Centre, Universiti Teknologi Malaysia, Johor Bahru 81310, Johor, Malaysia

\*e-mail: [suryanidyah@fst.unair.ac.id](mailto:suryanidyah@fst.unair.ac.id)

**Abstract.** *Staphylococcus aureus* (*S. aureus*) can form biofilms that contribute to antibiotic-resistant infections. This study investigated the effectiveness of a combined red diode laser (665 nm) and ozone system for inactivating *S. aureus* biofilms. Biofilm samples were treated with ozone, laser irradiation, or a combination of both, and bacterial survival was evaluated after incubation. Statistical analysis was performed using a factorial ANOVA test. The results demonstrated that combined laser irradiation with a power density of 0.24 W/cm<sup>2</sup> and ozone treatment significantly enhanced biofilm inactivation compared to either treatment alone. The maximum biofilm reduction reached 94% with combined treatment during 40 s, compared to less than 80% reduction using laser irradiation alone. These findings indicate that red diode laser and ozone combination therapy is a promising approach for effectively reducing *S. aureus* biofilms, offering potential advantages for managing antibiotic-resistant infections.

**Keywords:** biofilm; *Staphylococcus aureus*; red diode laser (665 nm); ozone; percent reduction.

Paper #9431 received 12 Nov 2025; revised manuscript received 15 Jan 2026; accepted for publication 17 Jan 2026; published online 19 Mar 2026. [doi: 10.18287/JBPE26.12.010304](https://doi.org/10.18287/JBPE26.12.010304).

## 1 Introduction

Tropical regions are significantly impacted by infectious diseases due to microorganisms that invade the body and lead to illness [1]. Key vectors include viruses, fungi, bacteria, and parasites. Major entry points for bacteria are the respiratory and gastrointestinal tracts, as well as the genitals and urine tract [2]. Approximately 10% of hospital patients develop nosocomial infections, with *Staphylococcus aureus* (*S. aureus*) being a prevalent cause, transmitted through food, medication, medical equipment, or healthcare personnel [3]. The term “staphylococcus”, derived from Greek, describes these gram-positive, spherical bacteria that cluster like grapes and are found globally, including in soil [4].

The hospital utilizes sterilization facilities to reduce infection by eliminating spores and bacteria from surfaces. Spore bacteria are notably resistant to sterilization efforts [5]. Factors affecting sterilization effectiveness include the type and number of germs,

contamination levels, and instrument design features [6]. Dental tools, which must be sterilized, often use dry heat sterilization though this method has limitations such as slow penetration, high costs, and ineffectiveness with non-metallic instruments [7]. Autoclaves, employing high-temperature steam, are commonly used but require consistent heat and maintenance, and rely on boiling water to operate safely [8].

*S. aureus* bacteria frequently create biofilms on medical equipment [9]. A biofilm is a group of microbial cells that form an irreversible bond to a surface and are encased in a matrix of extracellular polymeric substances (EPS) that they independently produce [10]. Biofilms exhibit phenotypic changes from planktonic cells or their free cells, such as changes in growth rates and changes in gene transcription [11]. Bacteria are able to endure physical, chemical, and biological challenges when biofilms are present. Biofilms function by impeding immune system function and generating antibiotic

resistance [12, 13]. The photodynamic inactivation (PDI) approach is one of the most precise solutions needed to address the issue of resistance brought on by biofilms [14].

PDI is a therapeutic process involving light, photosensitizers, and oxygen, aimed at inhibiting the growth of disease-causing microorganisms [15]. It starts with photosensitization, primarily using porphyrins, which absorb light to produce reactive oxygen species (ROS) that can kill bacteria [16]. Different light sources, including lasers and LEDs, are employed in antimicrobial photodynamic therapy [17]. The mechanism involves photophysical, photochemical, and photobiological activities: porphyrins absorb light, excite electrons, and generate ROS upon interaction with oxygen, leading to bacterial cell death [18].

By using light that corresponds to the absorption spectra of porphyrin photosensitizers and appropriate irradiation doses, bacterial cells can be photoinactivated. Previous studies indicate that the photodynamic technique, utilizing diode laser light, produces both photobiomodulation and antimicrobial effects. Ozone, a minimal atmospheric component, is generated through ultraviolet light and dielectric plasma discharge and has been shown to effectively reduce various microorganisms, including bacteria, viruses, and fungi [19]. It is particularly effective in preserving horticultural products and preventing biofilm deterioration of *S. aureus*, with experiments showing a reduction of up to 71.96% in *S. aureus* biofilms at an effective ozone concentration of 0.01 mg/L. Combining ozone with photodynamic treatment enhances microbial inactivation through optimal ozone levels, laser energy, and exposure time [20].

PDI effectively combats biofilm-associated resistance by generating ROS through light, photosensitizers, and oxygen, damaging bacterial cells. Combining PDI with ozone enhances bacterial inactivation and weakens biofilm structures, leading to increased efficacy against *S. aureus* biofilms. The study focuses on developing a system that integrates red diode laser with controlled ozone flow, evaluating different laser energy doses and ozone durations to optimize bacterial eradication. This work aims to advance antimicrobial photodynamic therapy and improve infection control, particularly in high infectious disease regions.

## 2 Methods and Materials

### 2.1 Sample Extraction

Fresh leaves of binahong (*Anredera cordifolia*) and betel (Piper beetle) were collected in Sidoarjo, East Java, cleaned with distilled water, and prepared by removing the stalks. The leaves were blended with 70% ethanol in a 1:5 ratios (20 g of leaves to 100 ml of ethanol), and then subjected to maceration for seven days in a closed container. After filtering, the ethanol extract was stored at 4 °C for future experiments [21].

### 2.2 Bacterial Culture

*S. aureus* ATCC 25923 was inoculated on Tryptone Soy Agar and incubated at 37 °C, calibrated to 1.0 McFarland Standard (approximately  $10^8$  colony-forming units (CFU)/mL). The bacteria were transferred to Trypsin Soy Broth, diluted with saline, and vortexed, resulting in serial dilutions ( $10^{-2}$  to  $10^{-8}$  CFU/mL). A 2% sucrose solution was added for biofilm production in a microplate incubated for 48 h at 37 °C. After phosphate-buffered saline (PBS) washing, crystal violet solution was added, and another incubation was performed for 30 minutes, with optical density (OD) measured at 450 nm using an enzyme-linked immunosorbent assay (ELISA) reader to confirm the method's accuracy.

### 2.3 Comprehensive Assessment of Bacterial Viability and Biofilm Biomass

A complex methodology was employed to assess biofilm biomass and bacterial viability, focusing on *S. aureus*. Initial bacterial cultures were established at specific concentrations and injected into microplate wells with sucrose, followed by a 48-h incubation. Biofilms were stained with crystal violet, and optical density was measured using an ELISA reader. Additional techniques, including CFU counting, confocal laser scanning microscopy, and scanning electron microscopy, were utilized to further investigate biofilm survival and structure, providing crucial insights into treatment effectiveness.

### 2.4 Experimental Unit

The experiments were carried out at 25.5–25.6 °C using the setup shown in Fig. 1. The experimental unit used a Laserland model 650RM-100 continuous red laser diode (nominal output power 100 mW) and an ozone generator (capacity  $10 \text{ g} \cdot \text{h}^{-1}$ ). Laser and ozone delivery were synchronized using a microcontroller. Biofilm samples were cultivated in 96-well microplates (growth area approximately  $0.32 \text{ cm}^2$  per well). The laser spot area at the biofilm surface was adjusted by changing the microplate height using a stepper motor (Z) and fixed when the spot area reached  $\sim 0.13 \text{ cm}^2$ . Although the power meter/detector provides high readout resolution, the physical parameters relevant to the biological experiments are limited primarily by (i) laser output stability during experiments and (ii) the uncertainty in defining/measuring the laser spot size at the sample plane; therefore, all laser parameters used for biological-dose calculations are reported with two significant figures. Dose calculations used  $A = 0.13 \text{ cm}^2$ ; timing/position controlled; ozone titrated iodometrically.

### 2.5 Treatment of the Sample

Four groups were tested: control, ozone only, laser only, and laser + ozone. Biofilms were exposed for 10, 20, 30, or 40 s at a constant irradiance power density.

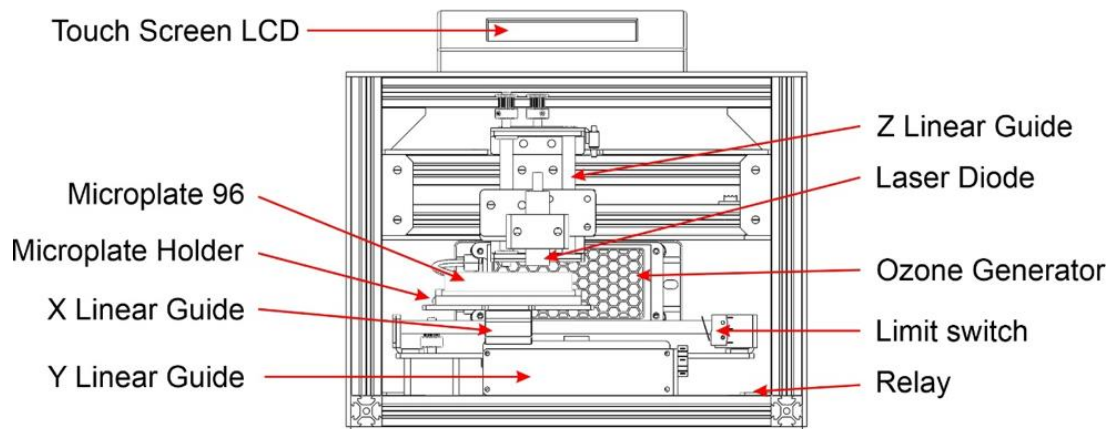


Fig. 1 Apparatus set-up of light and ozone source.

Two factors were analyzed: treatment modality and exposure time (10–40 s), with  $n = 5$  per condition. After treatment, samples were plated, incubated 24 h, and CFU were counted.

### 2.6 Data Analysis

A factorial two-way ANOVA test was employed in data analysis to evaluate how the therapy affected each group. The following Eq. (1) is then used to compute the percentage decrease in bacterial biofilm [22].

$$U_{exp} = n_1 \cdot n_2 + \frac{n_1 \cdot (n_1 + 1)}{2} - \sum r_1. \quad (2)$$

Optical density (OD) was used only as a supportive biofilm biomass and viability indicator; colony-forming units were the primary endpoint.

### 3 Results

Laser exposure was defined by the optical power at the sample plane and the exposure duration. The measured power ranged from 31.85–32.06 mW ( $\leq 2\%$  variation); therefore, all biological experiments and dose calculations use  $P = 32 \text{ mW} \pm 2\%$  (two significant figures), rather than time-specific power values. The monochromator spectrum peaked at 665 nm. Because of practical uncertainty in spot-size determination, the laser spot area used consistently was  $A = 0.13 \text{ cm}^2$ , giving an irradiance of  $E = 0.24 \text{ W/cm}^2$ . Biofilms were irradiated for 10–40 s, corresponding to  $H = 2.4\text{--}9.6 \text{ J/cm}^2$  ( $H = E \times t$ ). The previous table listing power/irradiance by exposure time was removed, and only the measured power range and nominal values used for biological calculations are reported.

Ozone was delivered to the sample through a fixed-output nozzle. The effective concentration of ozone, crucial for the effectiveness of treatment, was experimentally determined by collecting ozone in distilled water under identical conditions. The concentration was determined through iodometric titration using standardized sodium thiosulfate. Longer

exposure times resulted in higher concentrations of ozone. The results were summarized in Table 1. The error of the measurement method was  $\pm 5\%$  based on repeated trials ( $n=3$ ):

Table 1 Ozone concentration at various flow times.

| Flow time (s) | Concentration (mg/L) |
|---------------|----------------------|
| 10            | $1.5 \times 10^{-3}$ |
| 20            | $3.0 \times 10^{-3}$ |
| 30            | $4.0 \times 10^{-3}$ |
| 40            | $5.0 \times 10^{-3}$ |

The McFarland test was performed to determine the relationship between OD and bacterial concentration expressed as CFU/mL. OD values were measured using a UV-Vis spectrophotometer at 595 nm. To construct the calibration curve, CFU/mL values were obtained through the standard plate-count method: bacterial suspensions were serially diluted ( $10^{-1}$  to  $10^{-6}$ ), plated on TSA media, incubated for 24 h at 37 °C, and colonies within the 30–300 CFU range were counted. The colony count was then multiplied by the dilution factor to obtain the corresponding CFU/mL value for each OD measurement. Plotting OD against CFU/mL produced a linear relationship with  $R^2 = 0.98$ , indicating strong correlation. Fig. 2 shows the calibration curve of CFU/mL versus OD values at 595 nm.

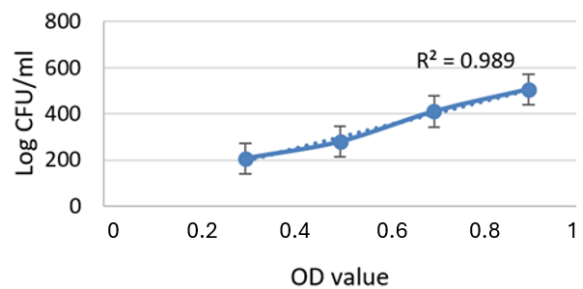


Fig. 2 Graph of the relationship between CFU/mL and OD values at a wavelength of 595 nm.

Table 2 Results of statistical analysis on *S. aureus* bacteria.

| Interaction            | 10         | <i>p</i> -value | 20         | <i>p</i> -value | 30         | <i>p</i> -value | 40         | <i>p</i> -value |
|------------------------|------------|-----------------|------------|-----------------|------------|-----------------|------------|-----------------|
| lasers vs ozone        | 36.21±2.76 | <0.001          | 50.98±2.17 | <0.001          | 60.22±1.61 | <0.001          | 70.41±1.94 | 0.001           |
| laser vs laser + ozone | 54.09±1.91 | <0.001          | 65.41±1.82 | <0.001          | 75.68±2.32 | <0.001          | 85.35±2.22 | <0.001          |
| ozone vs laser + ozone | 42.96±4.25 | <0.001          | 57.65±3.54 | <0.001          | 69.60±3.67 | <0.001          | 79.38±3.70 | <0.001          |

To ensure accurate quantification, dilutions yielding colony counts within the standard 30–300 CFU range were selected. Based on the serial dilution results, the 10<sup>-5</sup> dilution provided an average of 236 colonies, which met the acceptable counting range and was used to generate the corresponding CFU/mL value.

Treatment involved three groups exposed to different methods (laser, ozone, or both) for 10, 20, 30, or 40 s. The energy density varied with time increments, impacting the effectiveness as measured by percentage drops in OD or CFU/ml in bacterial biofilms. The results of the treatment in the three groups revealed a connection between the amount of time spent treating and the bacteria’s viability in the OD value shown in Fig. 3.

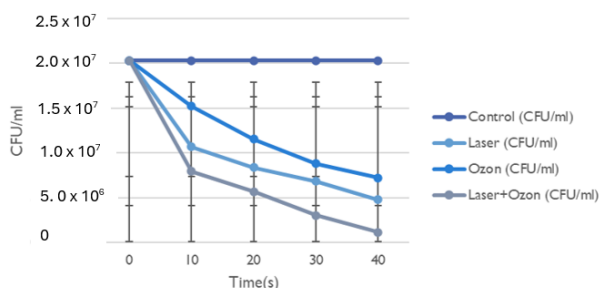


Fig. 3 Decreased biofilm viability of *S. aureus* bacteria.

The proportion of bacteria that died as a consequence of the calculation Fig. 4 displays the proportion of bacterial mortality.

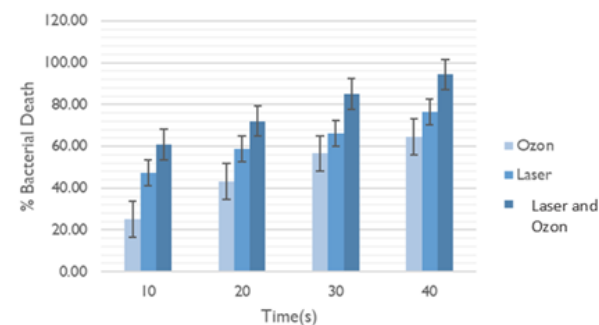


Fig. 4 Comparison of the percentage of *S. aureus* biofilm reduction.

The normality tests for the laser, ozone, and laser + ozone groups indicated normal distribution ( $p = 0.540$ ,  $p = 0.109$ ,  $p = 0.182$ ). Levene’s test confirmed homogeneity of variances ( $p > 0.05$ ). ANOVA results showed significant differences in treatment effectiveness over time for bacterial reduction, specifically for *S. aureus*, as detailed in Table 2.

By comparing the OD values across treatment groups, the percentage decrease was calculated. The OD readings were converted to estimated CFU/ml using the McFarland curve technique, and these converted values were then compared with the control group to determine the average percentage decrease. As the McFarland method has limited accuracy, these CFU/ml estimates should be interpreted with caution.

### 4 Discussion

Biofilms are clusters of microorganisms encased in an EPS that enhances their resistance to environmental factors, including antibiotics. The formation of a biofilm starts with an attachment phase and progresses through early (0–11 h), intermediate (12–24 h), and mature (24–48 h) stages (see, Fig. 5). As the biofilm matures, the EPS quantity increases, producing smaller pores that limit antibiotic penetration, especially during the adult phase [23]. As the biofilm becomes thicker and contains more EPS, the diffusion of light, photosensitizer, ozone, and reactive oxygen species becomes more limited. To manage the biofilm, one option is photodynamic treatment (PDT) [24].

PDT, utilizing red diode laser and ozone, demonstrates enhanced antibacterial effects against *S. aureus* biofilms [25]. The combination treatment generates reactive oxygen species (ROS), disrupting the extracellular polymeric substance matrix and bacterial membranes, allowing ozone to penetrate and induce oxidative damage [26]. This synergistic method leads to superior bacterial inactivation, with maximum reduction observed at 40 s [27]. The efficacy is attributed to photodynamic processes and ROS formation, with ozone contributing through oxidative actions and lipid peroxidation, highlighting the significance of ROS in compromising bacterial cell integrity [28, 29]. Illustration of the inactivation mechanism of *S. aureus* biofilms with red laser and ozone treatment is shown in Fig. 6.

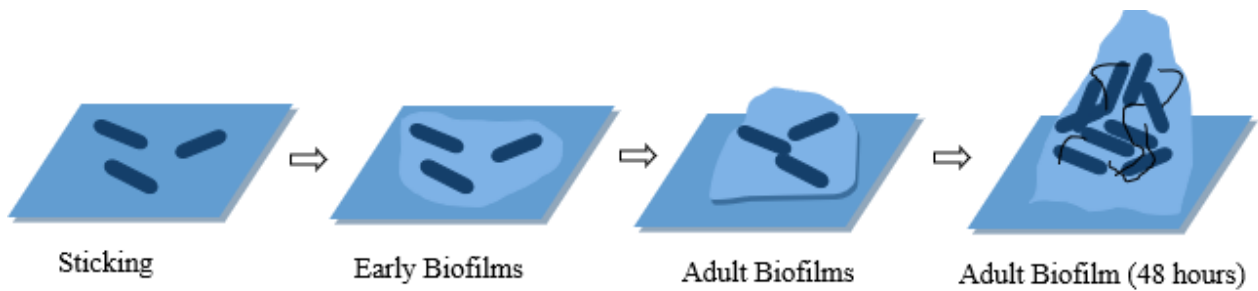


Fig. 5 Illustration of *S. aureus* Biofilm Growth Mechanism.

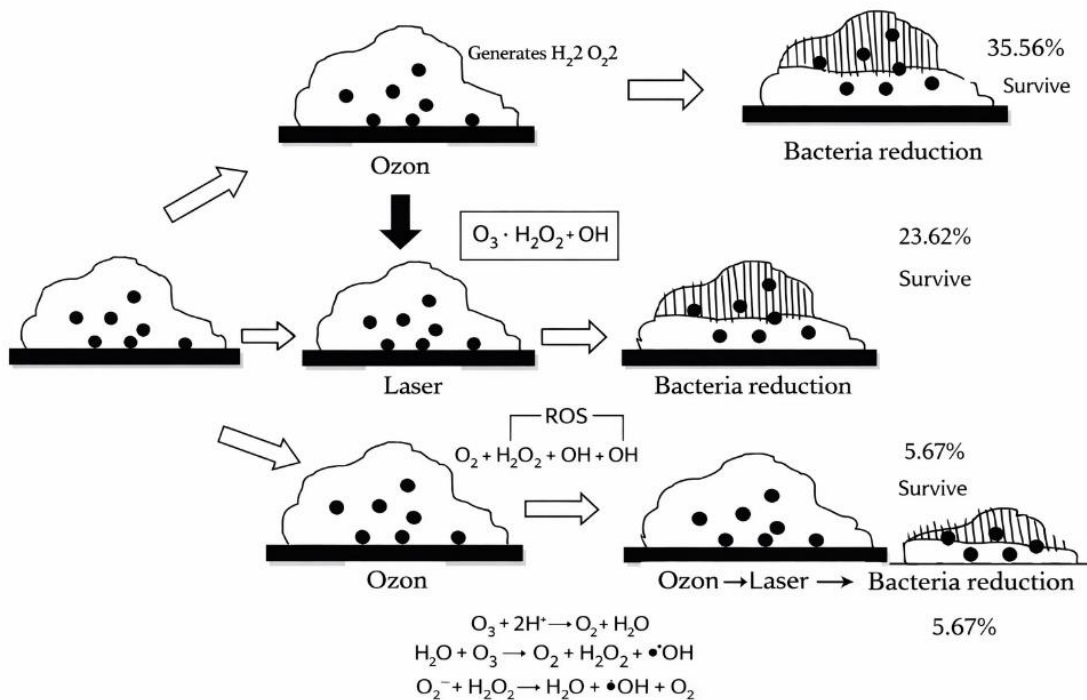


Fig. 6 Illustration of the inactivation mechanism of *S. aureus* biofilms with red laser and ozone treatment.

Ozone disrupts bacterial metabolism by inhibiting enzymes, effectively eliminating bacteria in biofilms. It reacts with polyunsaturated fatty acids to produce hydrogen peroxide (H<sub>2</sub>O<sub>2</sub>) [30]. Optimal ozone concentration is essential, as too little reduces effectiveness and too much can damage tissue. Consistent with the Results (Fig. 4), the highest bacterial reduction at 40 s was observed in the laser + ozone group (~94% reduction), which was higher than laser-only and ozone-only treatments. All percentage-reduction values discussed here follow the values presented in the Results figures and tables.

### 5 Conclusion

The outcomes demonstrated that ozone and a red diode laser worked together to lessen bacterial growth. The percentage decrease achieved by the laser therapy group alone increased by 29.89% when paired with ozone. This is due to ozone’s ability to trigger a process that results

in the production of H<sub>2</sub>O<sub>2</sub>, which increases the amount of harm done to bacterial biofilms. In this study, the maximum energy density for photo inactivating *S. aureus* biofilm was 9.6 J/cm<sup>2</sup> at 40 s with the addition of ozone, leading to a reduction percentage of *S. aureus* biofilm of 94%, as opposed to less than 80% at 40 s with laser alone. Thus, the *S. aureus* biofilm is effectively reduced by the red diode laser and ozone combination treatment.

### Acknowledgement

This research was funded by Airlangga Research Funds under the Doctoral Dissertation Research Scheme No. 1814/B/UN3.LPPM/PT.01.03/2025.

### Disclosures

All authors declare that there is no conflict of interest in this paper.

## References

1. J. L. Brooks, M. Jefferson, “[Staphylococcal biofi: lmsquest for the magic bullet](#),” *Advances in Applied Microbiology* 81, 63–87 (2012).
2. V. Neville, P. Dayan, I. D. Gilchrist, E. S. Paul, and M. Mendl, “[Using primary reinforcement to enhance translatability of a human affect and decision-making judgment bias task](#),” *Journal of Cognitive Neuroscience* 33(12), 2523–2535 (2021).
3. E. J. G. Pollitt, P. T. Szkuta, N. Burns, and S. J. Foster, “[Staphylococcus aureus infection dynamics](#),” *PLoS Pathogens* 14(6), e1007112 (2018).
4. S. D. Astuti, A. Zaidan, E. M. Setiawati, and Suhariningsih, “[Chlorophyll mediated photodynamic inactivation of blue laser on Streptococcus mutans](#),” *AIP Conference Proceedings*, 1718(1) (2016).
5. M. T. Mubarak, I. Ozsahin, and D. U. Ozsahin, “[Evaluation of sterilization methods for medical devices](#),” 2019 *Advances in Science and Engineering Technology International Conferences (ASET)*, 1–4 (2019).
6. P. DeSantis, “[Steam sterilization in autoclaves](#),” in *Handbook of Validation in Pharmaceutical Processes*, J. Agalloco, P. DeSantis, A. Grilli, and A. Pavell (Eds.), 4 Ed., CRC Press, Boca Raton, 217–230 (2021).
7. A. Blessing, S. I. Oluka, N. H. Nwobodo-Nzeribe, and C. H. Nwabueze “[Review of historical development of autoclave towards healthcare sector](#),” *International Journal of Real-Time Applications and Computing Systems* 2(3), 29–39 (2023).
8. A. K. Yaqubi, S. D. Astuti, A. H. Zaidan, A. Syahrom, and D. Z. I. Nurdin, “[Antibacterial effect of red laser-activated silver nanoparticles synthesized with grape seed extract against Staphylococcus aureus and Escherichia coli](#),” *Lasers in Medical Science* 39, 47 (2024).
9. S. D. Astuti, Hafidiana, R. Rulaningtyas, Abdurachman, A. P. Putra, Samian, and D. Arifianto, “[The efficacy of photodynamic inactivation with laser diode on Staphylococcus aureus biofilm with various ages of biofilm](#),” *Infectious Disease Reports* 12(s1), 8736 (2020).
10. A. K. Yaqubi, S. D. Astuti, P. A. D. Permatasari, N. Komariyah, E. Endarko, and A. H. Zaidan, “[In vitro inactivation efficiency of Bacillus subtilis and Escherichia coli bacteria in sterilizers using violet irradiation](#),” *Biomedical Photonics* 11, 4–10 (2022).
11. P. A. D. Permatasari, S. D. Astuti, A. K. Yaqubi, E. A. W. Paisei, and N. Anuar, “[Effectiveness of Katuk leaf chlorophyll \(Sauropus androgynus \(L.\) Merr\) with blue and red laser activation to reduce Aggregatibacter actinomycetemcomitans and Enterococcus faecalis biofilm](#),” *Biomedical Photonics* 12(1), 14–21 (2023).
12. K. Hoenes, U. Wenzel, B. Spellerberg, and M. Hessling, “[Photoinactivation sensitivity of Staphylococcus carnosus to visible-light irradiation as a function of wavelength](#),” *Photochemistry and Photobiology* 96(1), 156–169 (2020).
13. S. Astuti, V. Victory, A. Mahmud, A. Putra, and D. Winarni, “[The effects of laser diode treatment on liver dysfunction of Mus musculus due to carbofuran exposure: an in vivo study](#),” *Journal of Advanced Veterinary and Animal Research* 6(4), 499 (2019).
14. K. Plaetzer, B. Krammer, J. Berlanda, F. Berr, and T. Kiesslich, “[Photophysics and photochemistry of photodynamic therapy: fundamental aspects](#),” *Lasers in Medical Science* 24, 259–268 (2009).
15. S. D. Astuti, B. I. Prasaja, and T. A. Prijo, “[An in vivo photodynamic therapy with diode laser to cell activation of kidney dysfunction](#),” *Journal of Physics: Conference Series*, 853(1), 012038 (2017).
16. A. I. Mardianto, E. M. Setiawatie, W. P. Lestari, A. Rasheed, and S. D. Astuti, “[Photodynamic inactivation of Streptococcus mutans bacteria with photosensitizer Moringa oleifera activated by LED](#),” *Journal of Physics Conference Series* 1505(1), 012061 (2020).
17. D. Arifianto, S. D. Astuti, P. A. D. Permatasari, I. Arifah, A. K. Yaqubi, R. Rulaningtyas, and A. Syahrom, “[Design and application of near infrared LED and solenoid magnetic field instrument to inactivate pathogenic bacteria](#),” *Micromachines* 14(4), 848 (2023).
18. S. D. Astuti, R. A. Wibowo, N. I. D. N. Abdurachman, and K. Triyana, “[Antimicrobial photodynamic effects of polychromatic light activated by magnetic fields to bacterial viability](#),” *Journal of International Dental and Medical Research* 10(1), 111–117 (2017).
19. F. H. Quina, G. T. M. Silva, “[The photophysics of photosensitization: a brief overview](#),” *Journal of Photochemistry and Photobiology* 7, 100042 (2021).
20. D. M. Harris, J. G. Sulewski, “[Photoinactivation and photoablation of Porphyromonas gingivalis](#),” *Pathogens* 12(9), 1160 (2023).
21. A. Sułek, B. Pucelik, M. Kobielski, A. Barzowska, and J. M. Dąbrowski, “[Photodynamic inactivation of bacteria with porphyrin derivatives: effect of charge, lipophilicity, ROS generation, and cellular uptake on their biological activity in vitro](#),” *International Journal of Molecular Sciences* 21(22), 8716 (2020).
22. Suhariningsih, D. Winarni, S. A. Husen, F. Khaleyla, A. P. Putra, and S. D. Astuti, “[The effect of electric field, magnetic field, and infrared ray combination to reduce HOMA-IR index and GLUT 4 in diabetic model of Mus musculus](#),” *Lasers in Medical Science* 35, 1315–1321 (2020).

23. M. Piksa, C. Lian, I. C. Samuel, K. J. Pawlik, I. D. W. Samuel, and K. Matczyszyn, “[The role of the light source in antimicrobial photodynamic therapy](#),” *Chemical Society Reviews* 52(5), 1697–1722 (2023).
24. S. D. Astuti, W. I. Pratiwi, N. A. Tanassatha, K. A. Alamsyah, Y. Susilo, and M. Khasanah, “[Effect of ozone-induced diode laser of photodynamic inactivation on \*Pseudomonas aeruginosa\*](#),” *Malaysian Journal of Medicine and Health Sciences* 17(20), 27–32 (2021).
25. P. S. Puspita, S. D. Astuti, A. M. T. Nasution, A. A. S. Pradhana, and A. Mawaddah, “[Photodynamic therapy with ozone aids \*Staphylococcus aureus\* biofilm reduction](#),” *Indian Veterinary Journal* 97(2), 24–26 (2020).
26. S. Shui, Z. Zhao, H. Wang, M. Conrad, and G. Liu, “[Non-enzymatic lipid peroxidation initiated by photodynamic therapy drives a distinct ferroptosis-like cell death pathway](#),” *Redox Biology* 45, 102056 (2021).
27. S. D. Astuti, N. D. Drantantiyas, A. P. Putra, P. S. Puspita, A. Syahrom, and S. Suhariningsih, “[Photodynamic effectiveness of laser diode combined with ozone to reduce \*Staphylococcus aureus\* biofilm with exogenous chlorophyll of \*Dracaena angustifolia\* leaves](#),” *Biomedical Photonic* 8(2), 4–13 (2019).
28. U. Roobab, G. M. Madni, M. M. A. N. Ranjha, A. W. Khan, S. Selim, M. S. Almuhayawi, M. Samy, X.-A. Zeng, and R. M. Aadil, “[Applications of water activated by ozone, electrolysis, or gas plasma for microbial decontamination of raw and processed meat](#),” *Frontiers in Sustainable Food Systems* 7, 1007967 (2023).
29. S. D. Astuti, W. I. Pertiwi, S. P. A. Wahyuningsih, P. A. D. Permatasari, D. Z. I. Nurdin, and A. Syahrom, “[Effectiveness of ozone-laser photodynamic combination therapy for healing wounds infected with methicillin-resistant \*Staphylococcus aureus\* in mice](#),” *Veterinary World* 16(5), 1176–1184 (2023).
30. L. Rozykulyyeva, S. D. Astuti, A. H. Zaidan, A. A. S. Pradhana, and P. S. Puspita, “[Antibacterial activities of green synthesized silver nanoparticles from \*Punica granatum\* peel extract](#),” *AIP Conference Proceedings* 2314(1), 060012 (2020).